Kroon, D., Norris, R.D., and Klaus, A. (Eds.)
Proceedings of the Ocean Drilling Program, Scientific Results Volume 171B

2. PORE-WATER STRONTIUM ISOTOPES FROM THE LEG 171B DRILLING TRANSECT DOWN THE BLAKE SPUR[1]

William Ussler III,[2] Charles K. Paull,[2] and Paul D. Fullagar[3]

ABSTRACT

Strontium concentrations and ^{87}Sr/^{86}Sr values were measured on pore-water and sedimentary carbonate samples from sediments recovered at Sites 1049–1053 on the Blake Spur during Ocean Drilling Program Leg 171B. These sites form a 40-km-long depth transect extending along the crest of the Blake Spur from near the upper edge of the Blake Escarpment (a steep cliff composed of Mesozoic carbonates) westward toward the interior of the Blake-Bahama Platform. Although these sites were selected for paleoceanographic purposes, they also form a hydrologic transect across the upper eastern flank of the Blake-Bahama Platform. Here, we use pore-water strontium concentrations and isotopes as a proxy to define patterns of fluid movement through the flanks of this platform.

Pore-water strontium concentration increases with depth at all sites implying that strontium has been added during sediment burial and diagenesis. The isotopic values decrease from seawater-like values in the shallow samples (~0.70913) to values as low as 0.707342 in one of the deepest samples (~625 meters below seafloor). The change in pore-water strontium isotopic values is independent of the strontium isotopic compositions predicted from the host sediment age and measured on bulk carbonate in some samples. In most cases the difference between predicted sediment strontium isotopic composition and measured value is less than ±2 σ about the mean of the measured strontium value. Both the increase in concentration and the decrease in the strontium isotope values with increasing depth indicate that strontium was expelled from older carbonates. The strontium concentration and iso-

---

[1] Ussler, W. III, Paull, C.K., and Fullagar, P.D., 2000. Pore-water strontium isotopes from the Leg 171B drilling transect down the Blake Spur. *In* Kroon, D., Norris, R.D., and Klaus, A. (Eds.), *Proc. ODP, Sci. Results,* 171B, 1–17 [Online]. Available from World Wide Web: <http://www-odp.tamu.edu/publications/171B_SR/VOLUME/CHAPTERS/SR171B02.PDF>. [Cited YYYY-MM-DD]

[2] Department of Geological Sciences, University of North Carolina, Chapel Hill NC 27599-3315, USA.
Present address: Monterey Bay Aquarium Research Institute, 7700 Sandholdt Road, Moss Landing CA 95039-0628, USA. Correspondence author (Ussler): **methane@mbari.org**
[3] Monterey Bay Aquarium Research Institute, 7700 Sandholdt Road, Moss Landing CA 95039-0628, USA.

Initial receipt: 16 June 1999
Acceptance: 12 July 1999
Web publication: 11 August 2000
Ms 171BSR-118

tope profiles vary between sites according to their proximity to the Blake-Bahama Platform edge. Profiles from Site 1049 (nearest the platform edge) show the greatest amount of mixing with modern seawater, whereas the site most distal to the platform edge (Site 1052) shows the most significant influence of older, deeper carbonates on the pore-water strontium isotopic composition.

INTRODUCTION

The extent to which carbonate lithologies in the flanks of long-drowned shallow-water carbonate platforms are open or closed geochemical systems is not clearly known. Interstitial waters may still be nearly identical to primary connate waters, heavily altered by exchange with the host rock, or flushed by many volumes of seawater since their formation. Here, we assess the extent of fluid movement through the eastern flanks of the Florida-Bahama Platform using strontium as a tracer.

Fluid Movement in Analogous Carbonate Platforms

Many active carbonate platforms and atolls are known to have very fast flushing rates. Active circulation cells that involve seawater and may involve mixing with freshwater are common on the flanks of carbonate platforms (Kohout, 1967; Hanshaw and Back, 1980; Whitaker and Smart, 1990). Fluids in deep boreholes on Anewetak and Pikinni atolls oscillate on a tidal frequency (Swartz, 1958; Ladd and Schlanger, 1960; Aharon et al., 1987). Apparently, the interstitial waters deep within these emergent atolls are in open communication with the ocean. Boreholes into the tops of guyots in the Mid-Pacific Mountains indicate that the permeable parts of these long-drowned carbonate platforms are also flushed with modern seawater (Paull et al., 1995; Wilson et al., 1995).

Conversely, the interiors of some carbonate platforms contain fluids with distinct compositions that require restricted circulation for them to develop. For example, the Mesozoic rocks from the subaerial parts of the Florida-Bahama Platform contain pore waters with salinities of more than 200‰ (Manheim and Horn, 1968). Dense, brine-rich fluids believed to have been derived from the interior of the Florida-Bahama Platform are seeping out of the western flank of this platform along the base of the Florida Escarpment (Paull et al., 1991). The Florida Escarpment seeps are believed to be part of a large circulation cell that involves both seawater entering along the escarpment face and exiting the platform along the base of the escarpment. Similar circulation may occur along the face of the Blake Escarpment.

Many of the driving forces that stimulate fluid flow in emergent atolls or larger carbonate platforms (e.g., tidal forces, wave pumping, small changes in thermocline structure, hydrostatic heads associated with freshwater aquifers, and drainage associated with changes in sea level [Whitaker and Smart, 1990]) do not apply to their drowned counterparts. However, flow may be stimulated within drowned platforms by (1) lateral thermal differences that are developed by heat flow warming the interior of the platform (Kohout, 1967); (2) mixing with denser brines in the interior of the platform; (3) perturbations in the oceanic water column structure related to currents that flow around and over these structures; (4) paleoceanographically induced changes in the adjacent oceanic water column structure; and (5) diagenetic changes that alter pore-water density.

Regional Topography and Stratigraphy

During Ocean Drilling Program (ODP) Leg 171B, five sites were drilled along an ~40-km-long transect following the crest of the Blake Spur in water depths between 1344 and 2657 meters below sea level (Fig. **F1**) (Norris, Kroon, Klaus, et al., 1998). Middle to late Eocene-age pelagic carbonates covered with a thin phosphorite pavement crop out along the drilling transect. Most drill holes penetrated an expanded early Paleogene-age pelagic carbonate sequence and ended in Cretaceous-age carbonates.

F1. Cross section of Leg 171B drilling transect, p. 11.

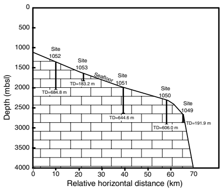

The Blake Spur is a prominent east- to west-oriented submarine headland that has developed between 1.5- and 5-km water depths along the otherwise north- to south-trending Blake Escarpment (Land et al., 1999). The slopes on the seaward edge of the Blake Spur between 2750- and 4800-m water depths are extremely steep (60°–80°). The Leg 171B transect (Fig. **F1**) extends from near the upper edge of the steep carbonate cliff updip toward the Blake Plateau and is associated with more gentle seafloor slopes (<5°).

The rocks exposed on the face of the Blake Spur (sampled between 2800 and 4000 m of water depth using the submersible *Alvin*) are composed of horizontally bedded Early Cretaceous-age carbonates of a shallow-water facies (Dillon et al., 1985). Regional seismic reflection profiles clearly show that these strata extend laterally under the Blake Spur and are in fact continuous with those underneath the Blake Plateau (Dillon and Popenoe, 1988).

Strontium Isotopes as Tracers of Fluid Circulation

Strontium is incorporated as a minor component (2000–10,000 ppm) during the formation of biogenic carbonates (Morse and MacKenzie, 1990). During normal burial diagenesis the strontium concentration in carbonate minerals decreases as they recrystallize. Thus, most ancient limestones have strontium concentrations of 200–600 ppm (Bathurst, 1975). The strontium lost by carbonate minerals undergoing recrystallization is transferred to the pore waters. Thus, carbonate diagenesis is one mechanism to elevate strontium concentrations in pore waters above the ~8 ppm strontium concentration that is characteristic of modern seawater. The isotopic composition of the strontium added to pore water by carbonate recrystallization will be the same as the biogenic carbonate from which it formed. Thus, by measuring differences between the $^{87}Sr/^{86}Sr$ values in pore waters and their host carbonates of known age, one can assess how much of the interstitial strontium is original and how much has been transported into the system (e.g., Baker et al., 1991; Elderfield et al., 1993).

Strontium isotope stratigraphies are based on the observation that the ocean is well mixed with respect to strontium and that carbonates, which form in ocean waters, reflect the isotopic composition of seawater. At the time of deposition, carbonates and the original pore water have the same isotopic values as the contemporaneous seawater (e.g., Burke et al., 1982; Hess et al., 1986; Ludwig et al., 1988). However, long-term changes in global chemical budgets slowly modify the strontium isotopic composition of the ocean (Brass, 1976). The general trends of seawater strontium isotopic composition ($^{87}Sr/^{86}Sr$) are well known back through the Cretaceous (Hess et al., 1986) with values of Early Cretaceous-age seawater (as monitored by the carbonates) <0.707 and modern seawater values >0.709.

The transect of sites drilled during Leg 171B (Fig. F1) is well suited for using strontium isotopes as a tracer of fluid circulation because (1) most of these carbonate-rich rocks have low clay content; thus, other sources of strontium that can make the interpretation of strontium isotope data equivocal (Elderfield and Gieskes, 1982) are reduced or eliminated; (2) the strontium isotopic compositions of the Lower Cretaceous-age carbonates and modern seawater are very distinct, and the change between these two time periods has been essentially unidirectional; and (3) the steep northern, eastern, and southern sides of the Blake Spur (Land et al., 1999) have exposed the strata within the spur to potential lateral flushing with seawater.

METHODS

Pore-Water Sample Collection and Storage

^{87}Sr/^{86}Sr analyses were conducted on pore-water samples obtained from drill cores collected at Sites 1049, 1050, 1051, 1052, and 1053 during Leg 171B (Fig. F1). Total penetration at these sites was 191.9, 606.0, 644.6, 684.8, and 183.2 m, respectively. Our samples were typically spaced between 10 and 25 m apart along the cores.

Whole-round sections of sediment were cut from the cores shortly after recovery on deck and extruded from the core liners, and the exterior of the sediment section was cut away to minimize seawater contamination. Pore water from this material was extracted using a hydraulic sediment squeezer. Shipboard pore-water chemical measurements are reported in Norris, Kroon, Klaus, et al. (1998). Water samples were split on shipboard and stored in flame-sealed glass ampoules for later analysis.

Strontium Isotopic and Concentration Analyses

Water samples originally stored in flame-sealed glass ampoules were transferred by pipette to Teflon vials and weighed to seven significant figures. After weighing, a ^{84}Sr spike was added to all samples for strontium concentration measurement and evaporated to dryness on a hot plate.

Sediment squeeze cakes were prepared for analysis by scraping or cutting the surface with a razor blade to remove possible surface contamination. An 8- to 20-mg portion of sample was weighed, and a known amount of ^{84}Sr spike was added. Approximately 1 mL of ultrapure 10% acetic acid was added to each sample in a Teflon vial. The sample was allowed to digest for 30 min in cold acid, and then centrifuged. The solution was removed by pipette and evaporated to dryness.

All samples were reacidified with 250 mL 5 N nitric acid, and the solution was loaded onto a preconditioned crown ether cation exchange resin (SrSpec). Columns were washed twice with 500 mL 5 N nitric acid, and strontium was collected with two separate aliquots of 500 mL Milli-Q water. Two mL of 1 N phosphoric acid was added, and the solution was dried on a hot plate.

Isotope ratio measurements were performed using a VG Sector 54 mass spectrometer in the Department of Geological Sciences at the University of North Carolina at Chapel Hill. Isotopic values have been normalized to $^{86}Sr/^{88}Sr = 0.1194$ using exponential normalization. The results for three to six (generally five) SRM-987 standards run in the same turret with unknowns were used to adjust the measured $^{87}Sr/^{86}Sr$ values of the unknowns; if 0.710250 was accepted as the correct value for the standard, and if the measured $^{87}Sr/^{86}Sr$ value for standards in a turret averaged 0.710245, then 0.000005 was added to the $^{87}Sr/^{86}Sr$ ratio for each sample in the turret.

Strontium concentrations (Fig. F2A) were computed using standard mass spectrometric isotope dilution techniques using the ^{84}Sr spike. Replicate analyses of standard samples indicate that strontium concentration measurements have an accuracy and precision better than 1% of the measured concentration.

F2. Strontium concentration vs. depth and sediment age, p. 12.

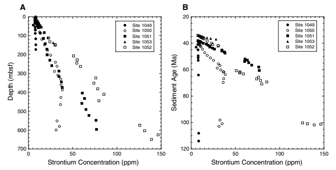

Host Sediment Ages

Host sediment ages were estimated using shipboard and shore-based refined biostratigraphic markers (Norris, Kroon, Klaus, et al., 1998). Assigned ages and their errors for nannoplankton and planktonic foraminifers within intervals between obvious sedimentation hiatuses were combined and plotted as a function of depth in each sediment core. A linear regression was fit to each selected depth interval and r^2 was generally >0.94. Predicted host sediment age was computed using the regression equation and depth in the sediment. Strontium isotope values for the host sediment were assigned using version 2 of the strontium isotope look-up table of Howarth and McArthur (1997).

RESULTS

Pore-Water Strontium Concentration

Except for the profile from Site 1050, pore-water strontium concentration increases linearly with depth (Table T1; Fig. F2A). However, the rate of the strontium concentration increase varies with depth along the Leg 171B transect (Fig. F1). Site 1049 shows the smallest increase with depth (from 7.2 to 8.4 ppm). The maximum measured concentration (~146 ppm) was at Site 1052, the site farthest away from the platform edge. In general, the strontium concentration gradient increases as the distance from the platform edge increases. At Site 1050 strontium concentration increases approximately linearly to a subsurface maximum at 386 meters below seafloor (mbsf). Below this level the concentration profile decreases slightly.

T1. Strontium concentration and isotope data, p. 16.

Pore-Water Strontium Isotopes

$^{87}Sr/^{86}Sr$ values decrease with depth at all Sites (Table T1; Fig. F3). In the shallowest samples the $^{87}Sr/^{86}Sr$ values are slightly less than our measurements of modern seawater (0.709175; Paull et al., 1995).

The depth profiles define a simple convex upward curvature in the three deeper holes (Sites 1050, 1051, and 1052). Strontium isotope values at these sites become nearly asymptotic to constant strontium isotopic values (Fig. F3). The profiles from Sites 1050 and 1051 are similar and both converge to basal $^{87}Sr/^{86}Sr$ values of 0.707775. The profile at Site 1052, which is farthest from the escarpment edge, converges on a slightly different basal value of 0.707400.

F3. Pore-water and sediment strontium isotopic composition vs. depth, p. 13.

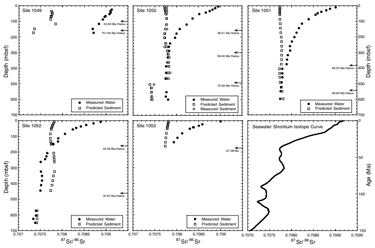

The isotope profile from Site 1049, nearest to the escarpment edge, is nearly linear and the values change less rapidly with depth compared to the other four sites. Drilling penetrated to only 183.3 mbsf at Site 1053, but the data from this site closely correspond with those from the upper portion of the adjacent Site 1052.

Sedimentary Carbonate Strontium Isotopes

The strontium isotopic composition of acid-leached sediment squeeze cakes from Site 1050 (Table T1; Fig. F3) correspond closely with the strontium isotopic composition predicted using biostratigraphy and the strontium seawater curve of Howarth and McArthur (1997). Figure F3 shows that 15 out of 25 predicted strontium isotopic compositions fall within 2 σ of the measured value (typically 0.000018), and no predicted $^{87}Sr/^{86}Sr$ value differed by more than 0.000094 (<7 σ of measurement at 502.72 mbsf). The differences between predicted and measured strontium isotopic values are not only the result of analytical errors but include the more subjective determination of biostratigraphic age.

DISCUSSION

Strontium Enrichment with Depth in the Sediment

Observed increases in strontium concentration with depth can be explained by either release of strontium from carbonate recrystallization (closed system) or transport of strontium into the strata from a region of higher concentration (open system), or a combination of both. The systematic increase in the strontium concentration with depth and distance from the Blake Escarpment (Fig. F2A) suggests that pore-water strontium concentration is increasingly dominated by local recrystallization and/or transport of high-strontium fluids from interior portions of the platform. An increase in pore-water strontium concentration caused by carbonate recrystallization should be a function of sediment age or burial depth. However, neither factor provides a simple explanation for the concentration data. Concentration profiles in Figure F2 show that pore-water strontium is independent of burial depth and sediment age. Sediments exposed at the seafloor are approximately late Eocene to early Oligocene in age and have strontium concentrations and isotopic compositions (Fig. F3) nearly the same as modern seawater. This indicates that the modern seafloor is an erosional feature that has been exposed for a sufficient amount of time to allow extensive chemical exchange in the upper sediment column. Thus, transport of strontium either by diffusion or advection must supplement local diagenetic release of strontium to the pore water.

Predicted vs. Measured Host Sediment $^{87}Sr/^{86}Sr$ Values

The strontium isotopic composition of the acid-leachable sedimentary carbonate was measured on all squeeze cakes from Site 1050 to determine whether the biostratigraphically determined strontium isotopic value is an accurate predictor for the actual isotopic value of the sedimentary carbonate. The results for Site 1050 (Fig. F3) show a close agreement between predicted and measured values. Apparently, clay minerals have not released measurable amounts of exotic strontium to the pore water. Thus, we interpret the differences between measured pore-water strontium isotopic compositions and those predicted for the host sediment as being caused by transport of strontium.

Differences between Predicted Host Sediment $^{87}Sr/^{86}Sr$ and Corresponding Pore-Water Values

The largest differences in the measured $^{87}Sr/^{86}Sr$ values of the pore water and the predicted $^{87}Sr/^{86}Sr$ composition of the host sediment generally occur at the seafloor, and the difference diminishes with depth (Fig. F3). However, the patterns are slightly different among the sites. At Site 1049 the largest difference in $^{87}Sr/^{86}Sr$ is seen at the bottom of the hole. In the three deeper holes (Sites 1050, 1051, and 1052), the pore-water and predicted host sediment $^{87}Sr/^{86}Sr$ values converge or cross (Fig. F3). Site 1053 values are similar to Site 1052, but the depth at Site 1053 is significantly less.

At Site 1050, both the measured pore-water $^{87}Sr/^{86}Sr$ values and the predicted $^{87}Sr/^{86}Sr$ composition of the host sediment converge within a zone between 300 and 500 mbsf that comprises Eocene-age sediment (Fig. F3). Below 500 mbsf the predicted host sediment $^{87}Sr/^{86}Sr$ values decrease abruptly below a 24-m.y. hiatus that separates Eocene-age from Cretaceous-age sediments. In this interval the measured pore water contains strontium values of ~0.707775. The zone below 300 mbsf also experiences a decrease in strontium concentration (Fig. F2). The three deepest pore-water samples at Site 1050 have $^{87}Sr/^{86}Sr$ values that are clearly distinct from the host sediment but similar to pore waters in overlying sections. This suggests that a major portion of the strontium has been derived from Eocene-age sediments that overlie the unconformity, rather than from older sediments below. The seawater strontium isotope curve (Fig. F3) shows that deeper sediments contain strontium of lower isotopic values and are unlikely sources for the strontium found in the deepest sediments drilled at Site 1050.

Site 1051 shows a simple profile (Fig. F3). The measured pore-water $^{87}Sr/^{86}Sr$ values converge with the nearly constant predicted $^{87}Sr/^{86}Sr$ values of the Eocene-age host sediments at ~400 mbsf.

Patterns of differences in the measured $^{87}Sr/^{86}Sr$ values of the pore water and the predicted $^{87}Sr/^{86}Sr$ composition of the host sediment at Site 1052 show variations with depth. From the seafloor to 160 mbsf pore-water $^{87}Sr/^{86}Sr$ values converge with the host sediment $^{87}Sr/^{86}Sr$ values. Between 160 and 460 mbsf the pore-water values are distinctly below those of their Eocene-age host sediments. However, in the four deepest samples (between 580 and 650 mbsf) the pore waters and their Cretaceous-age sediments have similar $^{87}Sr/^{86}Sr$ compositions. The strontium in the pore waters between 160 and 460 mbsf is apparently derived from stratigraphically Early Cretaceous-age strata.

The commonly observed discrepancies (Table T1) between the $^{87}Sr/^{86}Sr$ values measured in the pore waters and predicted for the host sediments from all sites along the transect argues against the Blake Spur sediments being a simple closed system with respect to strontium over geologic time.

Mixing

A composite isotope-mixing diagram (1/Sr concentration vs. isotopic composition; Faure, 1977) for the pore-water strontium measurements shows a linear array of points for each of the sites (Fig. F4). This linear

F4. Pore-water strontium isotopic composition vs. reciprocal strontium concentration, p. 15.

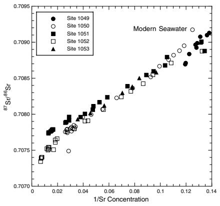

relationship indicates that simple two-component mixing can explain the range of pore-water strontium isotope values and concentrations spanning the drilling transect. The low concentration strontium end-member resembles modern seawater concentration and isotopic composition; however, individual trends are slightly different, reflecting differences in the source of the high concentration strontium end-member. At Site 1050 the values at the highest concentration (~37 ppm) indicate an Eocene-age end-member ($^{87}Sr/^{86}Sr$ = 0.707750). Regression lines for Sites 1051 and 1052 (Fig. **F4**) indicate that at source concentrations equal to the highest concentrations measured, the potential end-member strontium isotopic values are 0.707735 and 0.707340, respectively. The minimum ages of these presumed sources, based on the strontium isotope seawater curve of Howarth and McArthur (1997), are late Eocene (Sites 1050 and 1051) and mid-Cretaceous (Site 1052).

SUMMARY AND CONCLUSIONS

Pore-water strontium concentrations generally increase with depth and distance from the Blake-Bahama Platform edge. The measured strontium isotopic values of pore waters are commonly independent of host sediment age and burial depth. This indicates that the pore waters have exchanged strontium with one or more sources of different age. A comparison of measured and predicted strontium isotopic compositions indicates that the assumption that biostratigraphic ages are an accurate predictor of sedimentary carbonate strontium isotopic composition and is valid for these sediments, and that clay mineral diagenesis has not introduced exotic strontium to the pore water.

Strontium isotope and concentration profiles indicate complicated patterns of strontium redistribution. The data are not dense enough to define the overall circulation patterns uniquely. However, data from all the sites indicate that strontium from modern seawater has invaded the upper 100–300 mbsf enough to significantly alter the profile shapes. The greatest amount of seawater invasion is seen at Site 1049, which is directly at the platform edge. The reversal in the strontium concentration profile and the isotopic values at Site 1051 indicate that strontium has migrated downward (or at least laterally) from intermediate levels. At Site 1052, the site furthest from the escarpment, Mesozoic strontium appears to have moved upward into the Tertiary strata.

ACKNOWLEDGMENTS

Funding from JOI-USSAC supported this work. We thank Chieh Peng, John Lee, Kristina Faul, and Paul Wilson for their help at sea collecting and archiving the pore-water samples. Jon Martin provided a thoughtful review.

REFERENCES

Aharon, P., Socki, R.A., and Chan, L., 1987. Dolomitization of atolls by seawater convection flow: test of a hypothesis at Niue, South Pacific. *J. Geol.,* 95:187–203.

Baker, P.A., Stout, P.M., Kastner, M., and Elderfield, H., 1991. Large-scale lateral advection of seawater through oceanic crust in the central equatorial Pacific. *Earth Planet. Sci. Lett.,* 105:522–533.

Bathurst, R.G.C., 1975. *Carbonate Sediments and Their Diagenesis* (2nd ed.): Amsterdam (Elsevier).

Brass, G.W., 1976. The variation of the marine $^{87}Sr/^{86}Sr$ ratio during Phanerozoic time: interpretations using a flux model. *Geochem. Cosmochim. Acta,* 40:721–730.

Burke, W.H., Denison, R.E., Hetherington, E.A., Koepnick, R.B., Nelson, H.F., and Otto, J.B., 1982. Variation of seawater $^{87}Sr/^{86}Sr$ throughout Phanerozoic time. *Geology,* 10:516–519.

Dillon, W.P., Paull, C.K., and Gilbert, L.E., 1985. History of the Atlantic continental margin off Florida: the Blake Plateau basin. *In* Poag, C.W. (Ed.), *Geologic Evolution of the United States Atlantic Margin:* New York (Van Nostrand Reinhold), 189–215.

Dillon, W.P., and Popenoe, P., 1988. The Blake Plateau basin and Carolina Trough. *In* Sheridan, R.E., and Grow, J.A. (Eds.), *The Atlantic Continental Margin, U.S.* Geol. Soc. Am., Geol. of North America, I-2:291–328.

Elderfield, H., and Gieskes, J.M., 1982. Sr isotopes in interstitial waters of marine sediments from Deep Sea Drilling Project cores. *Nature,* 300:493–497.

Elderfield, H., Swart, P.K., McKenzie, J.A., and Williams, A., 1993. The strontium isotopic composition of pore waters from Leg 133: northeast Australian margin. *In* McKenzie, J.A., Davies, P.J., Palmer-Julson, A., et al., *Proc. ODP, Sci. Results,* 133: College Station, TX (Ocean Drilling Program), 473–480.

Faure, G., 1977. *Principles of Isotope Geology* (2nd ed.): New York (Wiley).

Hanshaw, B.B., and Back, W., 1980. Chemical mass-wasting of the northern Yucatan Peninsula by ground-water dissolution. *Geology,* 8:222–224.

Hess, J., Bender, M.L., and Schilling, J.G., 1986. Evolution of the ratio of strontium-87 to strontium-86 in seawater from Cretaceous to Present. *Science,* 231:979–984.

Howarth, R.J., and McArthur, J.M., 1997. Statistics for strontium isotope stratigraphy: a robust LOWESS fit to the marine Sr-isotope curve for 0 to 260 Ma, with look-up table for the derivation of numerical age. *J. Geol.,* 105:441–456.

Kohout, F.A., 1967. Ground-water flow and the geothermal regime of the Floridian Plateau. *Trans. Gulf Coast Assoc. Geol. Soc.,* 17:339–354.

Ladd, H.S., and Schlanger, S.O., 1960. Drilling operation on Enewetak Atoll. *Geol. Surv. Prof. Pap. U.S.,* 260Y:863–905.

Land, L.A., Paull, C.K., and Spiess, F.N., 1999. Abyssal erosion and scarp retreat: Deep Tow observations of the Blake Escarpment and Blake Spur. *Mar. Geol.,* 160:63–83.

Ludwig, K.R., Halley, R.B., Simmons, K.R., and Peterman Z.E., 1988. Strontium-isotope stratigraphy of Enewetak Atoll. *Geology,* 16:173–177.

Manheim, F.T., and Horn, M.K., 1968. Composition of deeper subsurface waters along the Atlantic continental margin. *Southeast. Geol.,* 9:215–236.

Morse, J.W., and Mackenzie, F.T., 1990. *Geochemistry of Sedimentary Carbonates:* Amsterdam (Elsevier).

Norris, R.D., Kroon, D., Klaus, A., et al., 1998. *Proc. ODP, Init. Repts.,* 171B: College Station, TX (Ocean Drilling Program).

Paull, C.K., Chanton, J.P., Martens, C.S., Fullagar, P.D., Neumann, A.C., and Coston, J.C., 1991. Seawater circulation through the flanks of the Florida Platform: evidence and implications. *Mar. Geol.,* 102:265–279.

Paull, C.K., Fullagar, P.D., Bralower, T.J., and Röhl, U., 1995. Seawater ventilation of Mid-Pacific guyots drilled during Leg 143. *In* Winterer, E.L., Sager, W.W., Firth, J.V., and Sinton, J.M. (Eds.), *Proc. ODP, Sci. Results,* 143: College Station, TX (Ocean Drilling Program), 231–241.

Swartz, J.H., 1958. Geothermal measurements on Enewetak and Bikini Atolls: Bikini and nearby Atolls. *Geol. Surv. Prof. Pap. U.S.,* 260-U:711–739.

Whitaker, F.F., and Smart, P.L., 1990. Active circulation of saline ground waters in carbonate platforms: evidence from the Great Bahama Bank. *Geology,* 18:200–203.

Wilson, P.A., Opdyke, B.N., and Elderfield, H., 1995. Strontium-isotope geochemistry of carbonates from Pacific guyots. *In* Haggerty, J.A., Premoli Silva, I., Rack, F., and McNutt, M.K. (Eds.), *Proc. ODP, Sci. Results,* 144: College Station, TX (Ocean Drilling Program), 447–457.

Figure F1. A diagrammatic cross section of the Leg 171B drilling transect illustrating the relative position of drill sites. Total depth (TD) is shown for each drill hole sampled for strontium concentration and isotopic measurements. The transect trends ~247° updip along seismic line TD-5 between DSDP Site 390 and the ASP-3 borehole (Dillon and Popenoe; 1988, fig. 1). Note that Sites 1052 and 1053 along the transect were drilled in reverse order.

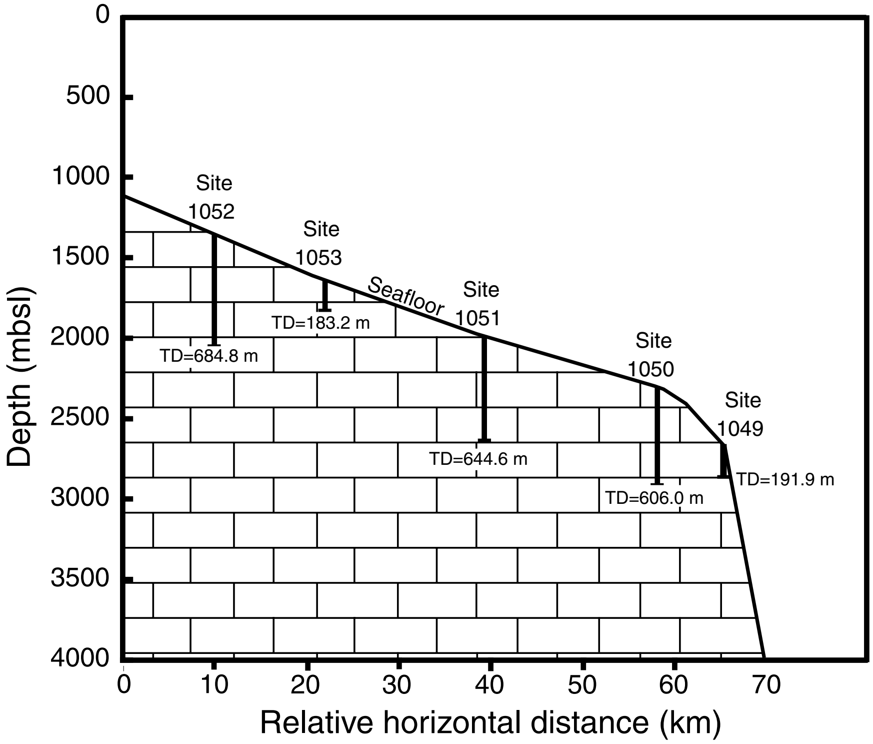

Figure F2. Pore-water strontium concentration plotted as a function of (**A**) depth and (**B**) host sediment age for each site sampled during Leg 171B. Concentration was measured using an isotope dilution method (see "**Strontium Isotopic and Concentration Analyses,**" p. 4, in "Methods"). Host sediment age was determined by shipboard biostratigraphy (Table **T1,** p. 16).

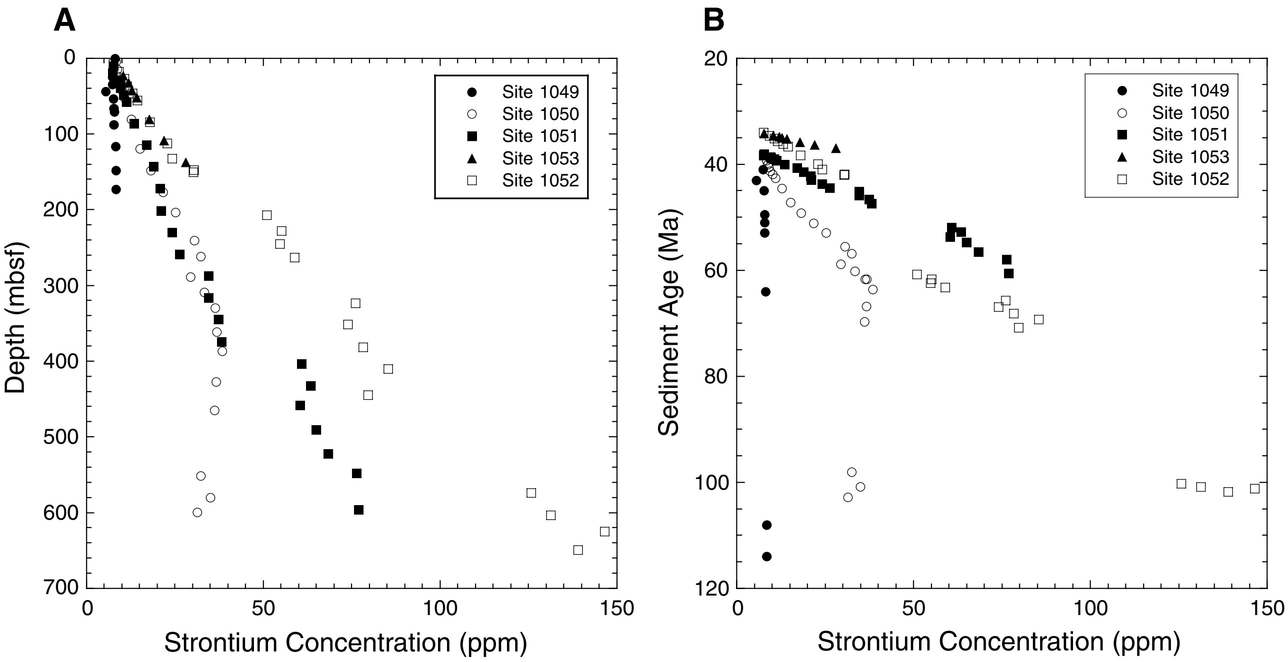

Figure F3. Measured strontium isotopic composition of pore waters and sedimentary carbonate (Site 1050 only) and predicted sediment strontium isotopic composition plotted as a function of depth for each drill site. Predicted sediment strontium isotopic compositions were estimated from biostratigraphic markers and the strontium look-up table of Howarth and McArthur (1997). The symbol diameter for the measured values of Site 1050 sediment is slightly smaller than two standard deviations (±2 σ) about the mean. For comparison, a composite seawater strontium isotopic curve derived from the 0- to 206-Ma curve published by Howarth and McArthur (1997) is also illustrated. Significant sedimentary hiatuses determined using shipboard biostratigraphy (Norris, Kroon, Klaus, et al., 1998) are indicated for each hole to provide a time context. (**Figure shown on next page.**)

Figure F3. (Caption on previous page.)

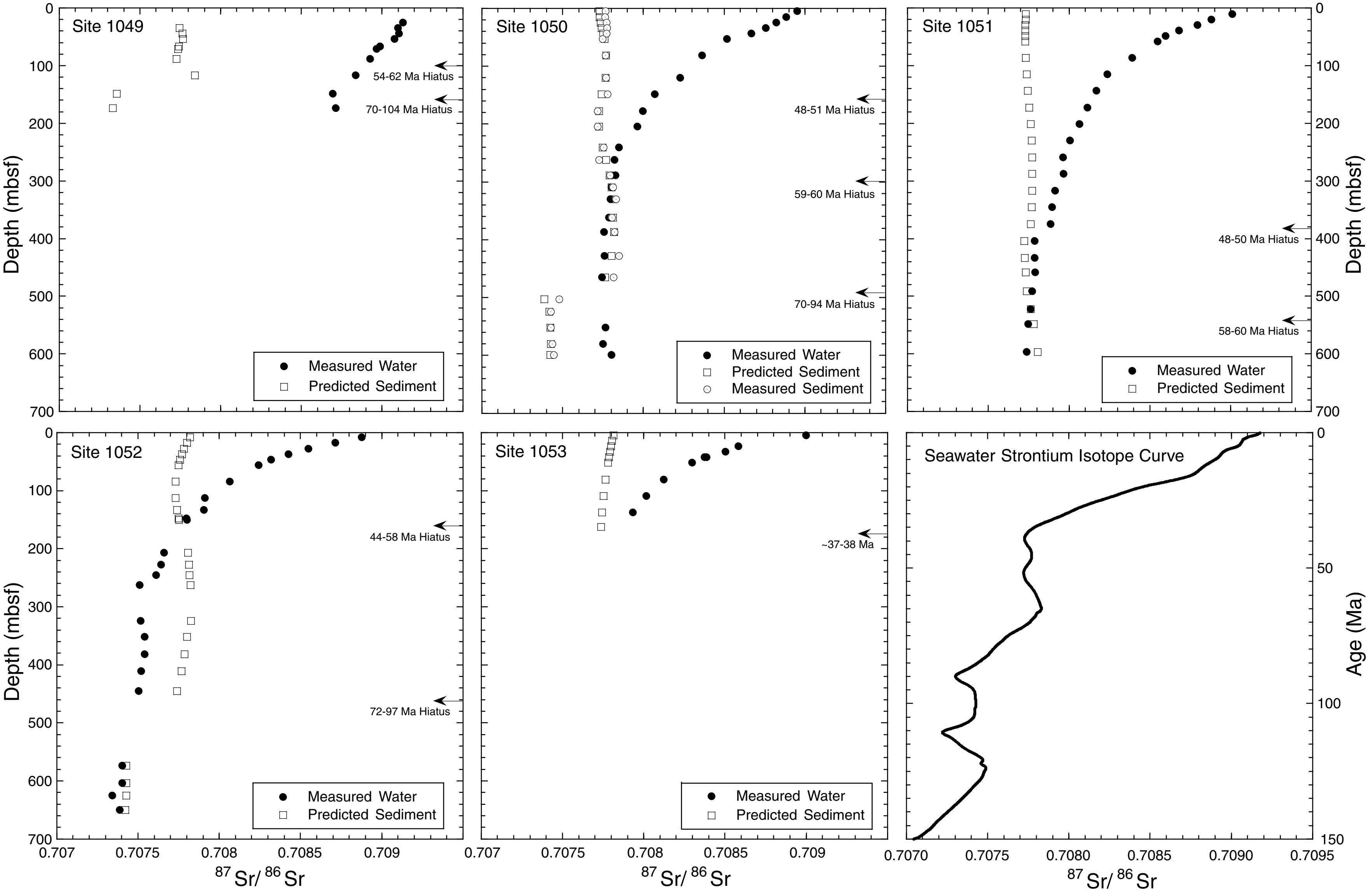

Figure F4. Pore-water strontium isotopic composition plotted as a function of reciprocal strontium concentration. The linear array for each drill site indicates that most of the variation of strontium isotopic values result from mixing between two distinct sources: a low strontium concentration end-member with modern seawater-like characteristics ($^{87}Sr/^{86}Sr$ = ~0.7092) and a high concentration end-member with either a late Eocene-age (Sites 1050 and 1052) or mid-Cretaceous–age (Site 1052) source with $^{87}Sr/^{86}Sr$ values at ~0.70774 and ~0.70734, respectively.

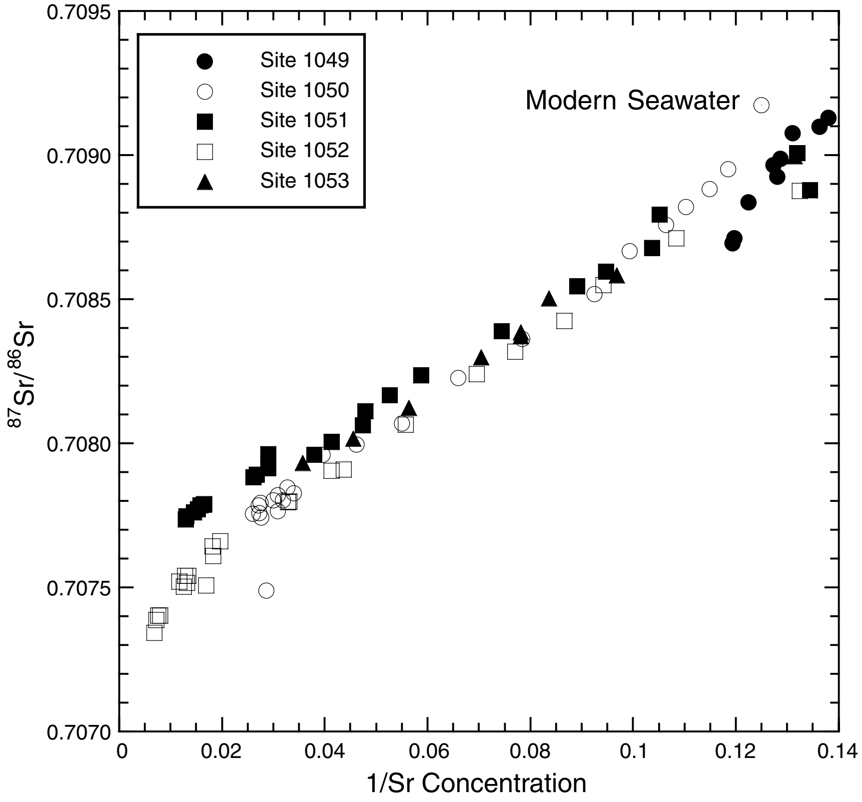

Table T1. Strontium concentration and isotope composition for pore waters and sedimentary carbonates, Leg 171B. (See table notes. Continued on next page.)

Core	Depth (mbsf)	Pore-water strontium concentration (µg/L)	Measured pore-water $^{87}Sr/^{86}Sr$	Sedimentary carbonate $^{87}Sr/^{86}Sr$	Strontium isotope pore-water age (Ma)	Host sediment age (Ma)
171B-1049A-						
3H	25.05	7.24	0.709128		1.21	–
4H	34.55	7.33	0.709098		1.70	41.0
5H	44.05	5.45	0.709105		1.53	43.0
6H	53.55	7.63	0.709076		2.60	45.0
9H	66.35	7.77	0.708986		6.16	49.5
10X	70.85	7.85	0.708966		6.61	51.0
12X	87.55	7.81	0.708924		9.03	53.0
16X	116.45	8.16	0.708836		12.38	64.0
19X	148.35	8.38	0.708695		16.91	108.0
22X	173.40	8.35	0.708712		16.47	114.0
171B-1050A-						
1X	4.45	8.44	0.708951	0.707763	7.04	39.3
2H	14.55	8.70	0.708882	0.707762	10.50	40.0
3H	24.05	9.07	0.708821	0.707772	12.80	40.6
4H	33.55	9.40	0.708757	0.707775	15.59	41.3
5H	43.05	10.06	0.708667	0.707772	17.20	41.9
6H	52.55	10.82	0.708517	0.707747	19.08	42.6
9H	80.62	12.75	0.708362	0.707764	21.60	44.5
13X	119.25	15.16	0.708228	0.707769	24.29	47.2
16X	148.05	18.16	0.708069	0.707777	27.54	49.2
19X	176.85	21.63	0.707995	0.707714	29.52	51.1
22X	203.60	25.23	0.707961	0.707715	30.47	53.0
26X	240.60	30.60	0.707848	0.707753	33.19	55.5
29X	261.30	32.36	0.707820	0.707724	33.94	56.9
32X	288.60	29.43	0.707826	0.707793	33.78	58.8
35X	309.30	33.27	0.707803	0.707811	34.42	60.2
171B-1050C-						
2R	330.00	36.32	0.707794	0.707828	34.70	61.7
5R	361.56	36.78	0.707786	0.707805	34.97	61.7
8R	386.24	38.38	0.707756	0.707821	36.26	63.6
13R	427.64	36.66	0.707759	0.707849	36.11	66.8
17R	464.65	36.17	0.707742	0.707812	37.13	69.7
21R	502.72			0.707479		93.4
23R	523.72			0.707425		95.5
26R	551.25	32.36	0.707764	0.707426	35.86	98.1
29R	580.05	34.96	0.707490	0.707435	36.65	100.9
31R	599.25	31.36	0.707802	0.707444	34.44	102.8
171B-1051A-						
2H	10.25	7.58	0.709008		5.63	38.1
3H	19.75	7.44	0.708879		10.60	38.3
4H	29.25	9.50	0.708793		14.24	38.6
5H	38.75	9.64	0.708678		17.04	38.8
6H	48.25	10.56	0.708596		18.13	39.0
7H	57.75	11.23	0.708546		18.73	39.3
10H	86.25	13.43	0.708389		21.07	40.0
13H	114.75	17.02	0.708236		24.13	40.7
16H	143.2	18.96	0.708168		25.41	41.5
19X	172.2	20.87	0.708111		26.59	42.2
22X	201	21.09	0.708063		27.68	42.9
25X	229.8	24.19	0.708005		29.25	43.7
28X	258.6	26.29	0.707960		30.49	44.4
31X	287.4	34.52	0.707963		30.42	45.2
34X	316.2	34.55	0.707913		31.65	45.9
37X	345.1	37.34	0.707892		32.17	46.6
40X	374.1	38.18	0.707883		32.38	47.4
43X	403.9	60.83	0.707787		34.94	51.9
46X	432.7	63.41	0.707785		35.01	52.8
49X	458.5	60.36	0.707789		34.87	53.7
53X	490.5	64.96	0.707771		35.56	54.7
56X	522.25	68.34	0.707760		36.06	56.6
59X	548.05	76.34	0.707746		36.85	58.0
65X	596.15	76.94	0.707737		37.51	60.6

Table T1 (continued).

Core	Depth (mbsf)	Pore-water strontium concentration (µg/L)	Measured pore-water $^{87}Sr/^{86}Sr$	Sedimentary carbonate $^{87}Sr/^{86}Sr$	Strontium isotope pore-water age (Ma)	Host sediment age (Ma)
171B-1052A-						
2X	7.95	7.55	0.708876		10.70	34.0
3H	17.65	9.22	0.708712		16.51	34.6
4H	27.15	10.61	0.708549		18.69	35.1
5H	36.65	11.54	0.708425		20.42	35.6
6H	46.15	12.97	0.708318		22.49	36.2
7H	55.65	14.36	0.708241		24.04	36.7
10H	84.15	17.93	0.708065		27.63	38.3
13H	112.65	22.86	0.707910		31.73	39.9
16X	132.65	24.20	0.707905		31.85	41.0
18X	150.15	30.23	0.707799		34.54	42.0
171B-1052E-						
2R	147.33	30.38	0.707797		34.60	41.9
8R	206.85	50.93	0.707660		73.63	60.8
10R	227.6	55.10	0.707642		74.24	61.7
12R	245.09	54.70	0.707610		75.68	62.4
14R	262.79	58.87	0.707508		81.68	63.2
20R	323.65	76.02	0.707516		81.10	65.7
23R	351.18	73.94	0.707540		79.53	66.9
26R	381.45	78.24	0.707540		79.53	68.1
29R	410.25	85.34	0.707520		80.82	69.3
33R	444.63	79.59	0.707502		82.04	70.8
46R	573.61	125.73	0.707403		86.36	100.2
49R	603.17	131.25	0.707403		86.36	100.8
52R	624.55	146.44	0.707342		88.20	101.2
55R	649.25	138.87	0.707387		86.89	101.8
171B-1053A-						
1H	4.45	7.61	0.708997		5.80	34.2
3H	23.45	10.33	0.708582		18.31	34.6
4H	32.95	11.95	0.708502		19.27	34.8
5H	42.45	12.78	0.708372		21.41	35.0
	42.45	12.78	0.708385		21.15	35.0
6H	51.95	14.19	0.708298		22.92	35.2
9H	80.45	17.74	0.708123		26.33	35.8
12H	108.45	21.92	0.708016		28.95	36.4
15H	137.45	28.02	0.707931		31.21	37.0

Notes: Strontium isotope pore-water age was obtained using measured $^{87}Sr/^{86}Sr$ values and the strontium isotope look-up table of Howarth and McArthur (1997). Host sediment age was estimated using short linear regressions between hiatuses fit to age vs. depth plots derived from biostratigraphy. See **"Results,"** p. 5, for details.